Polymer 50 (2009) 1868–1876

Contents lists available at ScienceDirect

Polymer

journal homepage: www.elsevier.com/locate/polymer

Generation and characterization of carbon nano-fiber–poly(arylene ether sulfone) nanocomposite foams

Desmond J. VanHouten [a], Donald G. Baird [b,*]

[a] Macromolecular Science and Engineering, Virginia Polytechnic Institute and State University, Blacksburg, VA 24061-0211, USA
[b] Department of Chemical Engineering, Virginia Polytechnic Institute and State University, 133 Randolph Hall, Blacksburg, VA 24061-0211, USA

ARTICLE INFO

Article history:
Received 4 December 2008
Received in revised form
5 February 2009
Accepted 7 February 2009
Available online 13 February 2009

Keywords:
Carbon nano-fiber
Poly(arylene ether sulfone)
Foam

ABSTRACT

In this study, carbon nano-fibers (CNFs) were used to increase the compressive properties of poly(arylene ether sulfone) (PAES) foams. The polymer composite pellets were produced by melt blending the PAES resin with CNFs in a single screw extruder. The pellets were saturated and foamed with water and CO_2 in a one-step batch process method. Dynamic mechanical thermal analysis (DMTA) was used to determine the reduced glass transition temperature (T_g) of the CNF–PAES as a result of plasticization with water and CO_2. Sharp transitions were observed as peaks in the tan δ leading to accurate quantitative values for the T_g. By accurately determining the reduced T_g, the foaming temperature could be chosen to control the foam morphology. Foams were produced which ranged in density from 290 to 1100 kg/m^3. The foams had cell nucleation densities between 10^9 and 10^{10} cells/cm^3, two orders of magnitude higher than unreinforced PAES foam, suggesting that the CNFs acted as heterogeneous nucleating agents. The CNF–PAES foam exhibited improved compressive properties compared to unreinforced PAES foam produced from a similar method. Both the specific compressive modulus and strength increased by over 1.5 times that of unreinforced PAES foam. The specific compressive strength of 59 MPa for the CNF–PAES foam is similar to that of commonly used high performance structural foam, poly(methacrylimide foam).

1. Introduction

The development of lightweight, structural materials is important in aerospace, automotive, marine, rail, and wind energy applications [1]. Polymeric foams are gaining interest for use in these applications because they have a large strength to weight ratio, as well as being cost effective when compared to other lightweight, structural materials [2]. The compressive properties of foams are important because structural foams are often used in applications where compressive forces are applied. Poly(methacrylimide) (PMI) foams have high specific compressive strength properties, up to 67 MPa [1]. However, PMI is limited in it's upper use temperature, with the compressive properties greatly decreasing at temperatures above 177 °C.

In order to increase the strength to weight ratio of polymers, microcellular foams were developed [3]. Microcellular foams are characterized by having a cell size less than 10 μm and a cell nucleation density greater than 10^9 cells/cm^3. It was hypothesized that if the cell size of the foam was smaller than the critical flaw size of the polymer, the microcellular foam would maintain the mechanical properties of the polymer matrix while increasing the impact toughness [3,4].

In an effort to improve the mechanical properties of microcellular foams, microcellular nanocomposite foams have been produced by combining nano-clays and polymer matrices, including polystyrene [5–7], PMMA [5,6], polypropylene [7,8], polyethylene [9,10], and polyethylene–octene [11]. The nanocomposites produced were either intercalated and featured agglomerates of clay particles or were exfoliated and the nanoparticles were well dispersed throughout the polymer matrix. In all of the studies involving composites made using nano-clays, the addition of the particles improved the cell morphology of the foam. When the particles were present, heterogeneous nucleation was dominant, which led to cell morphology with a smaller cell size and an increased cell nucleation density. The cell size distribution was also narrowed when compared to the neat polymer foam. As long as the particles were exfoliated and well dispersed, even at low levels of nano-clays (0.5%), they were able to act as a heterogeneous nucleating agent leading to numerous small cells [5,6,12]. The dispersion of the nano-clays was the most important factor in the resulting microcellular foam structure. If the nano-clays were exfoliated and well dispersed, there was more surface area on which cells could nucleate. The resulting foam had small cell sizes and a large cell density.

* Corresponding author. Tel.: +1 540 231 5998; fax: +1 540 231 5022.
E-mail address: dbaird@vt.edu (D.G. Baird).

0032-3861/$ – see front matter © 2009 Elsevier Ltd. All rights reserved.
doi:10.1016/j.polymer.2009.02.005

The dispersion and exfoliation were also important for increasing the tensile and compressive properties of the nanocomposite foam. Two studies were performed, one involving polystyrene and one involving PMMA. The tensile properties of the nanocomposite foams were lower than the unfoamed polymer, regardless of the clay dispersion, even if the tensile properties were normalized to account for the lower density. However, the tensile properties were improved when compared to the neat polymer foam as long as good dispersion of the clays was observed [5,12]. The increase in the tensile properties of the nanocomposite foam was also attributed to the reinforcing nature of the clay. As the nanocomposites were foamed, the biaxial extension of bubble growth caused the nano-clays to orient. As a result, the nano-clays helped to reinforce the cell wall by aligning around the nucleated bubble. Transmission electron microscopy has been used to show this phenomenon in literature [7,8].

While nano-clays have been shown to improve the mechanical properties of several microcellular foams, incorporation of the nano-clays into polymers with high glass transition temperatures (T_g) is difficult. Nano-clays are often organically modified to enhance the dispersion in polymer matrices [13]. Cation surfactants, often alkylammonium or alkylphosphonium cations, are used to enhance the miscibility of the nano-clays with the polymer. However, these cation surfactants tend to degrade at the high temperatures necessary to melt process these polymers.

Carbon nano-fibers have also been incorporated into polymer matrices and then foamed using supercritical carbon dioxide as the foaming agent. Shen et al. [14,15] have studied the effect of incorporating carbon nano-fibers (0.3–5 wt.%) into polystyrene. By incorporating well-dispersed carbon nano-fibers into the polystyrene matrix, it was found that the nano-fibers were able to act as a heterogeneous nucleating agent. It was determined that the carbon nano-fibers exhibited a greater nucleating efficiency than the nano-clays. Thus, the carbon nano-fibers were able to nucleate more cells at a lower percent loading [15]. Like the nano-clays, the carbon nano-fibers were shown to align around the nucleated cell walls, leading to an increase in the tensile and compressive moduli of the nanocomposite foam when compared to the neat foam [14].

Both tensile and compressive properties of microcellular polystyrene foams which were reinforced with carbon nano-fibers (1 and 5 wt.% loading) were reported [14]. By incorporating carbon nano-fibers, the reduced tensile modulus of the carbon nano-fiber reinforced foam was greater than that of the neat polystyrene (both foamed and unfoamed) for both 1 and 5 wt.% loading of fibers. However, the tensile strength was lower for the reinforced foam, making the reinforced foams less ductile. The ductility decreased with an increased weight percent of fibers. To study the effect of the carbon nano-fibers on the compressive properties of the foam, two different density foams were produced (~80% reduction and ~50% reduction) with both 1 and 5 wt.% loading. The low density foam (~80% reduction) had a much lower compressive modulus than unfoamed polystyrene regardless of the amount of carbon nano-fibers. The medium density foam (~50% reduction) exhibited a compressive modulus that was higher than unfoamed polystyrene, with the values from the samples containing 1 and 5 wt.% nano-fibers being statistically indifferent. Both the tensile and compressive moduli of microcellular polystyrene foams reinforced with carbon nano-fibers were greater than those values of neat polystyrene.

Foams of poly(arylene ether sulfone) (PAES) have demonstrated relatively high compressive properties. Microcellular foams of PAES were first produced by Sun et al. [16,17]. Supercritical carbon dioxide ($scCO_2$) was used as the blowing agent to produce the microcellular foams in a two-step process. The two-step process yielded foam with cell sizes of 1–7 μm, cell nucleation density of 10^{11} cells/cm^3, and up to 60% reduction in bulk density. The resulting foams exhibited specific compressive properties which were reported to be greater than theoretical predictions. The actual values of the compressive strength and modulus were not reported.

VanHouten and Baird [18,19] introduced a new process for foaming PAES to further reduce the foam density. A one-step batch process was utilized with a dual plasticizer blowing agent system to produce the PAES foam. The process produced foam which had an average cell size of 54 μm, cell nucleation density of 10^7 cells/cm^3, and up to 80% reduction in foam density. The compressive strength and modulus were compared to several commercially available polymeric foams. The specific compressive modulus and strength were 913 MPa and 38 MPa, respectively. While the compressive strength was better than several of the commercially available structural foams, the compressive modulus was slightly lower.

The objective of this research was to determine whether foams produced from CNF reinforced PAES over a range of foam densities, would exhibit enhanced compressive properties, tensile modulus, and impact strength compared to the neat PAES foam [19]. Foams were produced which had cell sizes ranging from 1 to 100 μm and foam densities ranging from 290 to 1100 kg/m^3. Of primary concern here is the effect of the foam morphology on the compressive properties, tensile modulus, and impact strength of the CNF–PAES foams.

A second objective of this research was to more fully exploit the use of the blowing agents of water and CO_2, which both plasticize the polymer, to control the cell size and density. In particular, dynamic mechanical thermal analysis (DMTA) is utilized to more accurately determine the suppression of the T_g, when compared to differential scanning calorimetry, and thereby more carefully select temperatures at which foaming occurs.

2. Experimental

2.1. Materials

Poly(arylene ether sulfone) (PAES, Radel® R-5800) was generously supplied by Solvay Advanced Polymers (Alpharetta, GA). The glass transition temperature (T_g) and density of the polymer were 220 °C and 1.29 g/cm^3, respectively. Heat-treated, vapor grown carbon nano-fibers (PR-19-XT-LHT) were obtained from Pyrograf Products (Cedarville, OH). The fibers had an average diameter of 150 nm and a length of 50–200 μm. Carbon dioxide was obtained from Airgas, Inc.

2.2. Preparation of the PAES–CNF nanocomposite material

Prior to melt blending, the PAES pellets and carbon nano-fibers were weighed and dry mixed with an industrial blender. The mixture was dried at 100 °C for 18–24 h under vacuum to remove the moisture. The dried PAES and carbon nano-fibers were compounded with a Killion extruder (L/D = 18, barrel diameter = 25.2 mm, and variable screw diameter from 16.6 mm at the feed to 21.45 mm at the exit) with a temperature profile of 310 °C–330 °C–350 °C, a die temperature of 350 °C, and screw speed of 25 rpm. A 3 mm diameter capillary die was used to produce a strand. The strand was drawn down to a diameter of 1 mm, cooled in a 1 m water bath, and fed into a pelletizer.

2.3. Foaming procedure

The PAES foams were produced using a one-step batch process method. A cylindrical stainless steel mold measuring 3.0 cm in diameter by 12.5 cm in length was filled with the PAES resin and liquid water (a 2:1 w/v ratio was used for polymer:water). The mold

was placed inside a pressure vessel which was sealed and charged with a predetermined amount of carbon dioxide (4.5 MPa). The pressure vessel was heated to 265 °C causing the pressure to increase to between 10 and 11 MPa. A saturation temperature of 265 °C was used to facilitate the sintering of the pellets during the saturation process, yielding a foamed specimen without weld lines after the foaming process. The gas was allowed to diffuse into the PAES for 1 h. The temperature was decreased to the desired temperature (165–227 °C), and the pressure was increased to 10.3 MPa using a high pressure pump. The pressure vessel was held at the desired temperature for one hour to assure full saturation. The pressure was rapidly released (less than 2 s) and the mold was removed from the pressure vessel. The mold was allowed to cool to room temperature before removing the foamed specimen.

Several obstacles must be overcome to produce a foamed sample which is of sufficient size and shape for mechanical testing, when using a one-step batch processing method. Although foaming a preformed polymer sheet or plug would result in the strongest foam, the sample would have to be several millimeters thick which would require long saturation times. Minimizing the diameter of the pellets is desirable to reduce saturation time by decreasing the distance which the gas has to diffuse. However, individually foamed pellets must be sintered together during processing to provide a usable part. Therefore, a higher initial saturation temperature (265 °C) was chosen to facilitate sintering of the CNF–PAES composite pellets during the saturation process. Because the water and CO_2 plasticize the PAES matrix, the viscosity of the composite material at 265 °C was reduced enough to induce flow of the pellets. The flowing of the pellets caused the composite material to form a flat cylindrical sheet in the mold. Once foamed, the sample exhibited no visible weld lines from the sintered pellets as was determined from visual analysis of a fractured surface.

2.4. Thermal analysis

Differential scanning calorimetry (DSC), thermogravimetric analysis (TGA) and DMTA were conducted on CNF–PAES samples which had been saturated with water and carbon dioxide. CNF–PAES was saturated with $scCO_2$ and water at 265 °C and 10–11 MPa for 1 h. The temperature was cooled to 220 °C and pressure regulated to 10.3 MPa, and the sample was saturated for an additional hour. The temperature was cooled to room temperature to eliminate the loss of blowing agents due to foaming, and the CNF–PAES was removed from the vessel. The saturated specimen was immediately tested upon removal from the pressure vessel. However, experiments proved that no appreciable loss of blowing agents occurred when the saturated specimen was subjected to ambient temperature and pressure for up to an hour after release.

CNF–PAES plaques were compression molded, prior to saturation, for DMTA testing. A Carver Laboratory Press was used to produce 2 mm thick sheets of CNF–PAES. The polymer pellets were placed in a rectangular mold and placed inside of the press, which was heated to 300 °C. A pressure of 11.5 MPa was applied to the mold for 10 min. The mold was cooled to room temperature, and the plaque was removed.

A DSC (TA Instruments, model Q1000) was used to determine the T_g of the samples. Scans were conducted under nitrogen from −20 °C to 260 °C at a heating rate of 10 °C/min. High volume DSC pans with rubber seals (TA instruments) were used to minimize the loss of blowing agents during testing.

A TGA (TA Instruments, model Q500) was used to determine the amount of blowing agents present in the PAES resin. Samples were run from 25 °C to 600 °C at a heating rate of 10 °C/min in a nitrogen atmosphere.

DMTA was performed on a Rheometrics RMS-800. Strips measuring 45 mm long, 4 mm wide, and 2 mm thick were cut from the plaque of CNF–PAES that was saturated with water and CO_2. A dynamic torsional test was conducted at a frequency of 1 s^{-1} and 1% strain leading to the measurement of the storage (G') and loss (G'') moduli from which the $\tan\delta$ was determined as a function of temperature from 50 to 240 °C.

2.5. Foam density

The foam density was determined using the water displacement method. A foam specimen was weighed and submerged in water. The displaced water was measured to determine the volume of the foam. Because the foam has a thin skin layer on the surface and a predominately closed cell structure, water uptake is negligible during the measurements.

2.6. Determination of cell size and cell nucleation density from SEM imaging

The cell size and structure of the foamed polymer were determined using a Leo 1550 field emission scanning electron microscope (FE-SEM) operated at 5 kV. The foam specimen was freeze fractured and sputter coated with 20 nm of gold. The SEM images were analyzed using ImageJ (National Institute of Health) image processing software. Typically, micrographs containing 25–50 cells were used to determine the average cell diameter and 100–200 cells were used to determine the cell nucleation density.

The cell nucleation density, N_o, was calculated using the method reported by Kumar and Weller and given by Eq. (1) [20]. In Eq. (1), n is the number of cells in the micrograph, M is the magnification, A is the area micrograph in cm^2, and V_f is the void fraction of the foam. V_f can be estimated from Eq. (2), where D represents the average diameter of the cells.

$$N_o = \left(\frac{nM^2}{A}\right)^{3/2} \frac{1}{\left(1 - V_f\right)} \tag{1}$$

$$V_f = \frac{\pi}{6} D^3 \left(\frac{nM^2}{A}\right)^{3/2} \tag{2}$$

2.7. Tensile testing

The tensile modulus of the foam was determined using an Instron 4204 and ASTM D638 was used as a guide for testing. Due to sample size limitation the ASTM test method was not followed exactly. Five rectangular samples measuring 45 mm in length, 10 mm in width, and 3 mm in thickness were cut from a large specimen of the PAES foam. The gauge length was set to 20 mm and the samples were tested at a constant speed of 1.27 mm/min. The strain was calculated from the displacement of the crosshead. The modulus was determined by applying a least-squares fit through the initial linear region of the stress–strain curve. The modulus represents an average of five foamed specimens.

2.8. Compression testing

The compressive properties of the foam were measured using an MTS (model 826.75) 50,000 lbs servo hydraulic test system. ASTM D1621 was used as a guide for testing. However, due to sample size limitations, the test method was not followed exactly. Five cylindrical samples measuring 30 mm in diameter and 40 mm in length

were cut from a large specimen of the PAES foam and the foam properties were determined from the average of the five samples. A lathe was used to cut the samples to ensure the cuts were perpendicular to the cylinder wall. The samples were compressed at a rate of 2.5 mm/min. The strain was calculated from the displacement of the crosshead and the modulus was determined by applying a least-squares fit through the initial linear region of the stress–strain curve.

2.9. Impact testing

The impact strengths of the foams were determined using ASTM D256-06a as a guide. Five samples measuring 63 mm long, 12.7 mm wide, and 3.2 mm thick were cut from a large specimen of the PAES foam. A sharp notch was cut into the sample using a Tinius Olsen Model 899 specimen notcher (Horsham, PA) turning at a high rotational speed. The notched specimens were tested using a Tinius Olsen 897 machine (Horsham, PA). Because the specimens were thinner than the ideal ASTM thickness, care was taken to ensure the samples did not buckle during impact.

3. Results and discussion

The production of CNF–PAES foams using water and CO_2 as the blowing agents and the associated mechanical properties are addressed in three parts. First, the amount of blowing agents absorbed under various conditions and their plasticization of the CNF–PAES are considered. Secondly, based on the information obtained in the first part of the research, the conditions for foaming of the CNF–PAES to obtain various degrees of density reduction and cell size are discussed. In particular, results from DMTA helped to refine the foaming process by quantifying the plasticization of the CNF–PAES with the water and CO_2. By understanding the thermal transitions, foams were produced by releasing the pressure at varying temperatures to control the cell morphology and foam density. We then conclude this section with a presentation of the mechanical properties obtained for the CNF–PAES foams of various morphologies (cell size and densities).

3.1. Determination of CNF–PAES plasticization from the presence of water and CO_2

Thermogravimetric analysis was conducted to determine the amount of water and CO_2 that diffused into the CNF–PAES polymer composite during saturation. In order to induce a large thermodynamic instability during foaming, a large solubility is desired [21,22]. The CNF–PAES was prepared in a similar manner to previously reported techniques which exhibited a large solubility of water and CO_2 [19]. It is shown in Fig. 1 that ~7.6% of water and CO_2 were able to diffuse into the CNF–PAES matrix during the 2 h saturation time, at 10.3 MPa. Similar amounts of water and CO_2 were able to diffuse into the neat PAES [19]. Therefore, the addition of the CNFs does not affect the solubility or diffusivity of the water and CO_2 in the PAES matrix.

DSC was used to determine how much the T_g of the CNF–PAES polymer composite was reduced by the presence of the 7.6% water and CO_2. VanHouten and Baird [19] previously demonstrated that when PAES was saturated with water and CO_2, the lowered T_g due to plasticization was observed followed by an endothermic peak attributed to the loss of the blowing agents from the polymer matrix. Similar thermograms were observed with the CNF–PAES polymer composite. It is shown in Fig. 2 that the water and CO_2 (7.6%, Fig. 1) reduce the T_g of the CNF–PAES to approximately 160 °C. A large endothermic peak was observed directly after the T_g inflection. It was difficult to quantify the degree of suppression of the T_g of the polymer due to plasticization using DSC because the endothermic peak was much larger than the inflection due to the T_g.

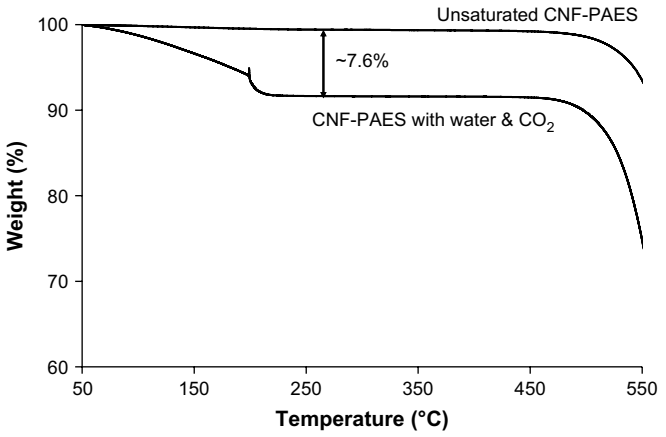

Fig. 1. TGA results of 1 wt.% CNF–PAES saturated with CO_2 and water. The TGA was run in a nitrogen atmosphere at a heating rate of 10 °C/min.

To better quantify the plasticization of the CNF–PAES with water and CO_2, DMTA was conducted. Dynamic torsional testing was conducted on strips of CNF–PAES. The storage modulus and tan δ are shown in Fig. 3 for CNF–PAES saturated with 7.6% CO_2 and water and CNF–PAES which had not been saturated. The data from the storage modulus suggests that the bulk of the sample remained saturated with the blowing agents until the CNF–PAES was heated to the lowered T_g due to plasticization. If a considerable amount of blowing agents were able to diffuse out of the CNF–PAES matrix, an increase in the storage modulus would be observed. Because no appreciable amount of blowing agents are lost during the DMTA testing of the PAES saturated with water and CO_2, DMTA was a viable option for quantitatively determining the plasticization of the polymer.

The T_g can be observed as either a rapid decrease in the storage modulus or a peak in the tan δ. The storage modulus and tan δ exhibited only one transition in the CNF–PAES samples containing no blowing agents. This transition was observed at 227 °C, which was close to the T_g of the PAES. When the CNF–PAES sample was saturated with CO_2 and water, three distinct transitions were observed as peaks in the tan δ. The first transition was observed at 160 °C, which is attributed to the plasticized T_g of the CNF–PAES

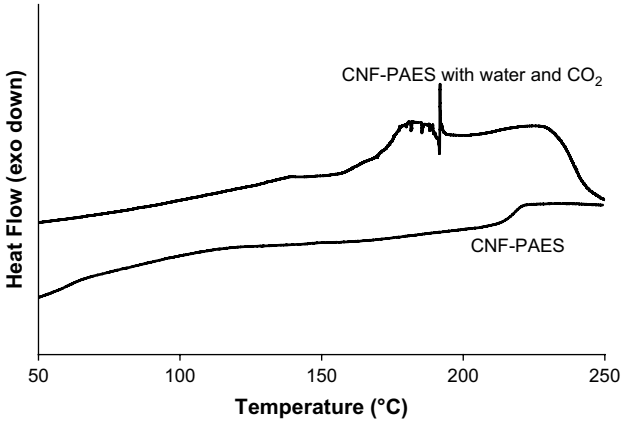

Fig. 2. DSC results of 1 wt.% CNF/PAES saturated with 7.6% $CO_2$and water. The DSC was run at a rate of 10 °C/min in a nitrogen atmosphere. The data has been shifted so the results could be seen more clearly.

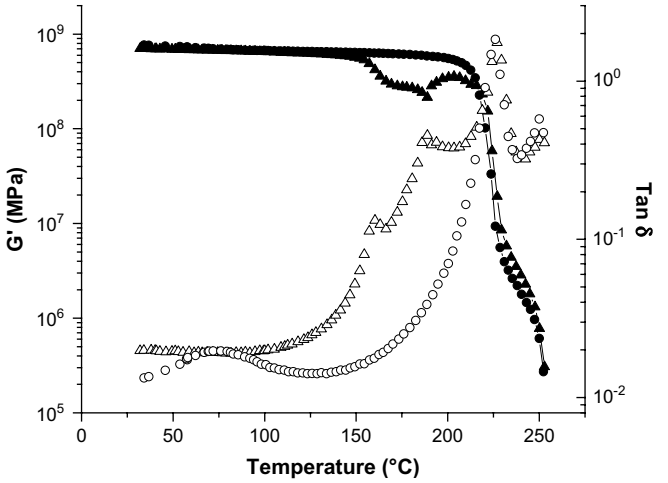

Fig. 3. DMTA results of 1 wt% CNF–PAES saturated with water and CO_2 (▲) and neat CNF–PAES (●). The closed symbols represent the storage modulus and the open symbols represent the tan δ. The DMA was run in a nitrogen atmosphere at a heating rate of 10 °C/min. The DMA was run at a frequency of 1 s^{-1} and 1% strain.

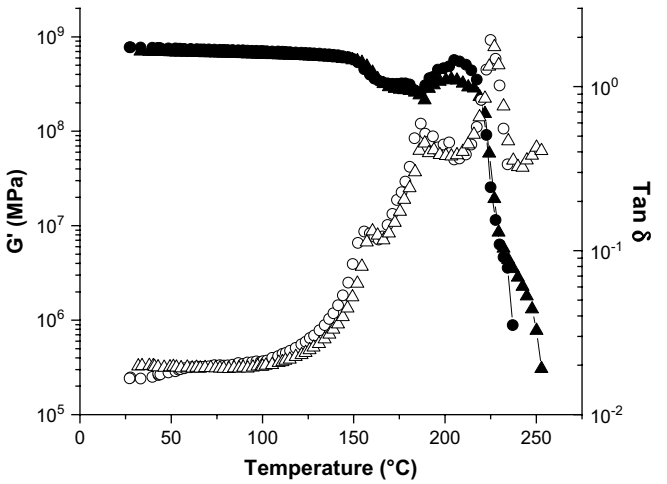

Fig. 4. DMTA results of 1 wt% CNF–PAES saturated for release at 165 °C (●) and 220 °C (▲). The closed symbols represent the storage modulus and the open symbols represent the tan δ. The DMA was run in a nitrogen atmosphere at a heating rate of 10 °C/min. The DMA was run at a frequency of 1 s^{-1} and 1% strain.

due to the presence of both the CO_2 and water. Once 160 °C was reached, the CO_2 was able to rapidly diffuse out of the PAES matrix while a majority of the water remained in the polymer. The broadening of the decrease in the storage modulus at 160 °C is due to the loss of the CO_2. This loss of CO_2 from the PAES matrix led to an increase in the T_g, which yielded another transition at 189 °C. This transition is attributed to the plasticized T_g due to water. Once 189 °C was reached, the water was able to escape by both diffusion and nucleation of bubbles from the PAES matrix. Because the water completely escaped from the PAES matrix, a transition at 227 °C was observed, which is the T_g of the CNF–PAES matrix without blowing agents.

DMTA was used to determine the effect of the release temperature on the diffusion and solubility of the blowing agents. During the saturation process, the temperature was decreased from 265 °C to the desired temperature for pressure release and held for an hour. Because the temperatures varied greatly, the solubility of the blowing agents could be affected. To prepare the DMTA samples, the CNF–PAES sample was saturated at 265 °C and 10.3 MPa for 1 h. The temperature was lowered to either 165 °C or 220 °C, the pressure regulated to 10.3 MPa, and CNF–PAES sample was saturated for an additional hour. The DMTA results for the samples saturated at 165 and 220 °C are shown in Fig. 4. From this figure, it can be seen that the decrease in temperature from 220 to 165 °C, for the last hour, does not affect the diffusion or solubility of the blowing agents as both curves exhibit the same transitions.

3.2. Characterization of foam morphology and density

Using blowing agents, which also plasticized the CNF–PAES, allowed for better control of the foam morphology. Samples were foamed at five different release temperatures to control the cell size and optimize the compressive properties of the foams. The release temperature is defined as the temperature of the pressure vessel at which the pressure was released. Temperatures were chosen based on the DMTA results ranging from nucleation with minimal cell growth (165 °C) to significant cell growth without foam collapse (227 °C). Release temperatures of 180 and 200 °C were chosen to assess the effect of the second observed T_g transition on the cell morphology. A release temperature of 220 °C was utilized so the foam morphology and mechanical properties could be compared to previously reported values of neat PAES foam produced from a similar process [19].

The SEM micrographs of these samples, shown in Fig. 5, show the effect foaming temperature had on cell morphology. It can be seen that as the foaming temperature is increased, cell size increases. When the release temperature is close to the plasticized T_g of the CNF–PAES, the cells do not have a lot of time to grow before vitrification is induced because the viscosity is becoming infinitely large. As the release temperature is increased, the cells have a longer time to grow and cell coalescence can occur, leading to larger diameter cells. Cell coalescence occurs when the growth of two or more cells impinge on each other and the cell walls become so thin that surface tension can no longer keep the cells separate. Evidence of cell coalescence can be seen in the SEM micrographs when the pressure was released at a temperature of 180 °C or higher. It is inferred that cell coalescence occurred because lines, which are indicative of coalesced cell walls, are observed in the larger cells. At the higher temperatures, cell coalescence occurs more frequently. Cell coalescence which led to macrocellular size cells occurred when the pressure was released at a temperature of 227 °C. Despite the cell coalescence at the higher temperatures, cells less than 1 μm are present for all temperatures. The number of the cells less than 1 μm decreases as the foaming temperature is increased.

The presence of a broad distribution of cell sizes can be seen in Figs. 5 and 6. In all of the micrographs, small cells (>1 μm) can be seen in the cell walls of the larger cells. The presence of distinctly different diameter cells suggests that there is more than one nucleation mechanism present during the foaming process. Upon rapid release of the pressure, the cells first nucleate due to the supersaturation of the CO_2 in the PAES matrix. Nucleation due to the supersaturation of the water occurs after the CO_2 nucleation. The bimodal distribution of cell sizes occurs because the two blowing agents nucleate the cells at different rates.

The DMTA confirms that two nucleation processes could occur during foaming when water and CO_2 are used as the blowing agents. The nucleation processes can be seen by the distinct transitions in the DMTA. At 160 °C, the CO_2 is able to be released from the PAES matrix. At this temperature, the CO_2 can begin to nucleate cells, while the water is still stable in the PAES matrix. When the temperature reaches 189 °C in the DMTA, the transition due to the water is observed. At this temperature, the water is unstable in the PAES matrix and can begin to nucleate cells. The difference in

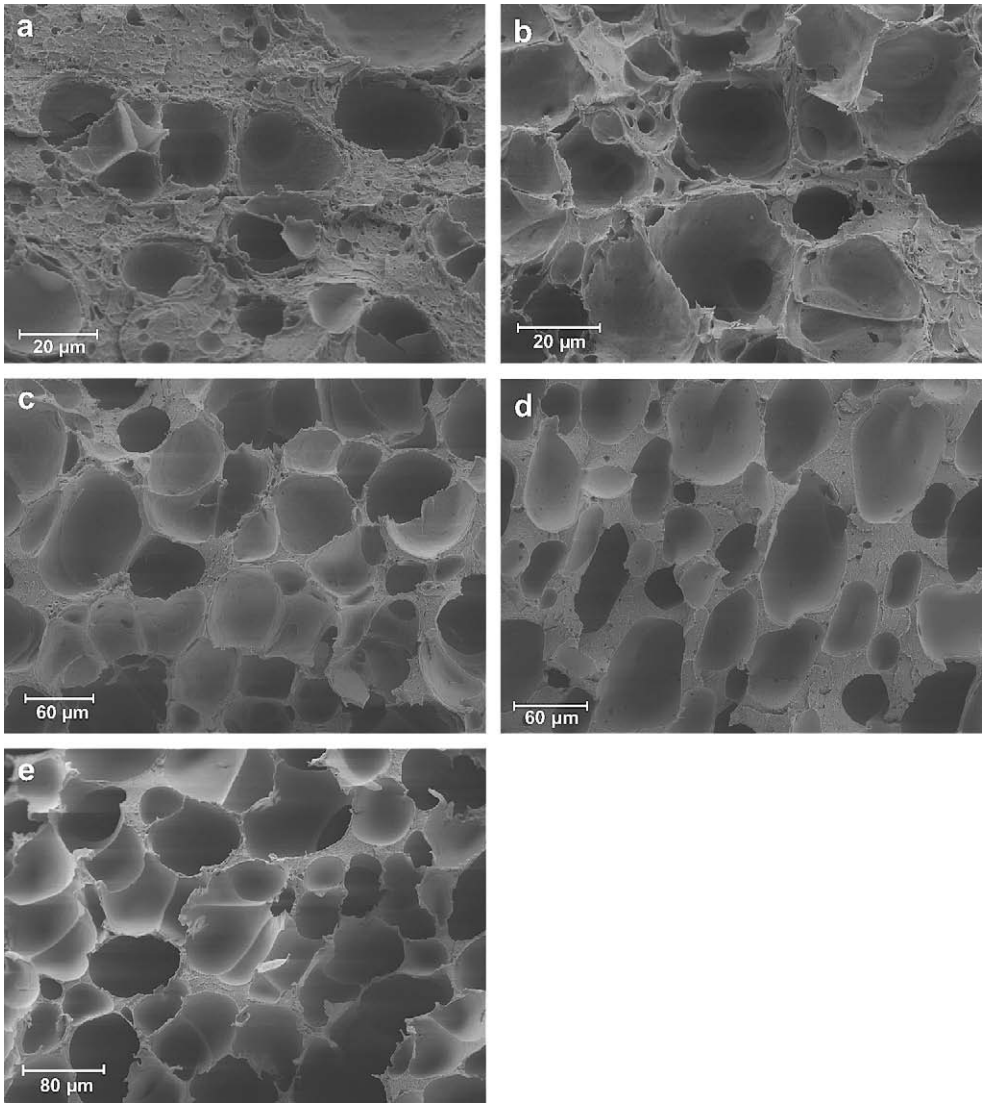

Fig. 5. SEM micrograph of the CNF–PAES foam produced from a one-step batch process utilizing water and CO_2 as the blowing agents at a release temperature of (a) 165 °C, (b) 180 °C, (c) 200 °C, (d) 220 °C, (e) 227 °C.

the stabilities of the blowing agents in the PAES matrix confirms that nucleation due to water and CO_2 occurs separately during the foaming process.

The cell nucleation density was calculated from the SEM micrographs, and it was determined that cell nucleation density was affected by the temperature at which the pressure was released. A plot of cell nucleation density is shown in Fig. 7. As the temperature of pressure release increased, the cell nucleation density decreased. The cell nucleation density decreased because of cell coalescence during the cell growth. As the cells grow together, the population of the cells decreases and this was observed as a decrease in the cell nucleation density.

For the CNF–PAES foam, the cell nucleation density ranged between 10^9 and 10^{10} cells/cm^3. The cell nucleation density was two orders of magnitude higher than neat PAES foam produced with water and CO_2 under the same saturation and foaming conditions [19]. The significant increase was attributed to the CNFs promoting heterogeneous nucleation. When heterogeneous nucleating agents are present, the activation energy of nucleation is significantly decreased so nucleation occurs much more easily, thus leading to a larger nucleation density [15,23]. Heterogeneous nucleation was observed in the SEM images and is shown in Fig. 8. In the micrograph, it can be seen that a CNF protrudes from the initially nucleated cell. The presence of heterogeneous nucleation produces a larger population of smaller cells, which can lead to better mechanical properties [14].

While the temperature of pressure release could be used to control the cell size, there was a tradeoff between cell size and the foam density. The effect of release temperature on the foam density is shown in Fig. 9. As the release temperature was increased, the foam density decreased. CNF–PAES foams were produced with a reduction in foam density ranging from 290 to 1100 kg/m^3, a 78–15% density reduction, by only controlling the temperature at which the pressure was released.

3.3. Determination of the tensile, compressive, and impact properties

The tensile, impact and compressive properties of the CNF–PAES foams were tested and are shown in Table 1. The temperature in the sample name refers to the release temperature at which the corresponding foam was produced. Previously reported values [19] for the

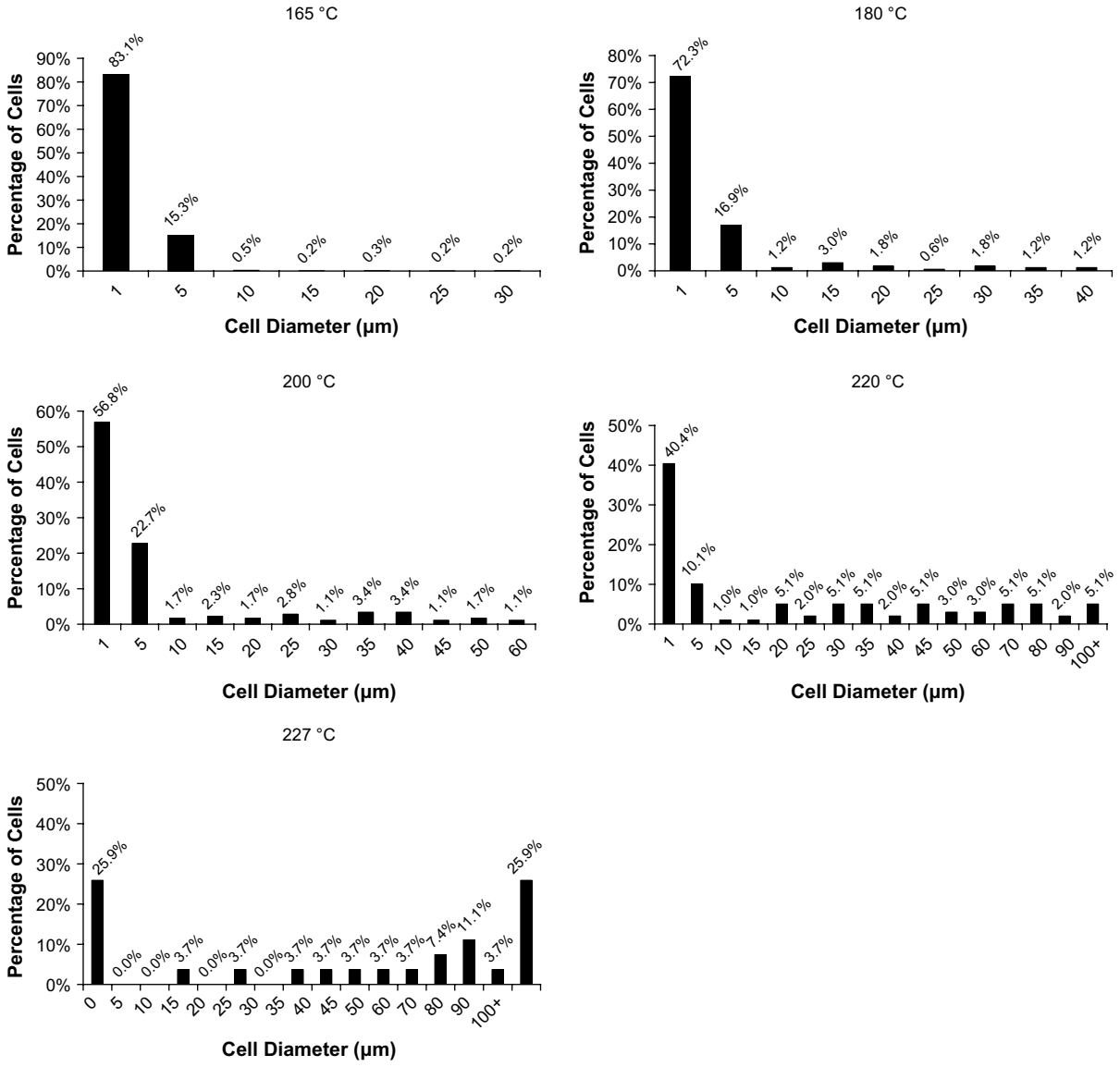

Fig. 6. Cell size distribution of the CNF–PAES foam saturated with water and CO_2 at 165 °C, 180 °C, 200 °C, 220 °C, 227 °C.

tensile, impact, and compressive properties of unreinforced PAES foam produced using water and CO_2 are also reported in Table 1 to determine the effect the CNFs had on the mechanical properties of the foams. All of the values are specific values, normalized by the foam density, to eliminate differences in the mechanical properties due to foam density. Because the samples were foamed in a cylindrical mold, the cells were oriented in the direction parallel to the cylinder wall.

The effect of both the cell morphology and the addition of the CNFs on the tensile modulus can be seen in Table 1. By comparing the PAES foam to the CNF–PAES foam (both foamed at 220 °C) it was determined that the addition of the CNFs yielded no effect on the foams because both foams exhibited tensile moduli which were statistically similar. Through comparison of the CNF–PAES foams produced at different release temperatures, the effect of the cell morphology on the tensile modulus of the foams was determined. The tensile modulus improved slightly as the cell size increased. As the foaming temperature was increased, up to 220 °C, the thickness of the cell walls also increased. The higher release temperature caused the cells with thin walls to coalesce. At a release temperature of 220 °C, a majority of the cell walls appeared to be greater than 1 μm, thus yielding a higher specific tensile modulus than the foams produced at the lower release temperatures. The increase in the cell growth, at a release temperature of 227 °C, led to a decrease in the cell wall thickness. The decrease in cell wall thickness led to a slight decrease in the specific tensile modulus. It should be noted that the improvement in the specific tensile modulus due to the foam morphology was minimal.

The addition of the CNFs to the PAES yielded foam which had a significantly lower specific notched izod impact strength. When compared to unreinforced PAES foam, the specific impact strength of the CNF–PAES foam decreased by approximately 40%. The decrease in the impact strength from the addition of the CNFs was due to the strengthening characteristics of the CNFs. The CNF–PAES was more rigid than the unreinforced PAES foam. The rigidity of the foam allowed energy transfer to occur more easily in the foam. Therefore, the sample did not recoverably deform, and little energy from the impact was lost due to deformation [24]. The cell morphology did not cause a statistically significant difference in the impact strength of the CNF–PAES foams.

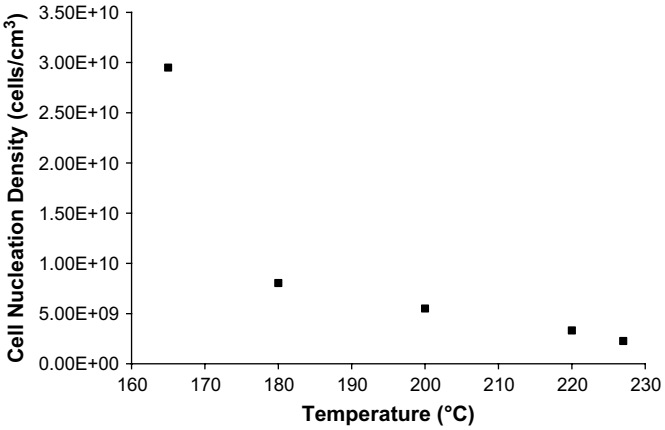

Fig. 7. Effect of the release temperature on the observed cell density for CNF–PAES foamed with water and CO_2.

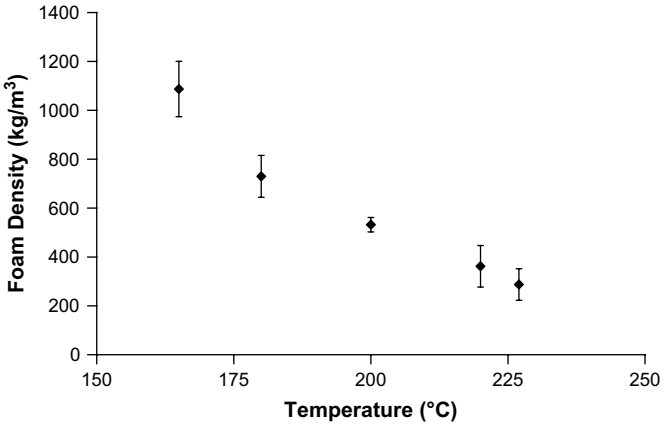

Fig. 9. Effect of foaming temperature on the bulk density of the CNF–PAES foams.

The compressive properties, modulus and strength, were most affected by the addition of the CNFs to the PAES. Both the specific compressive modulus and specific compressive strength increased over 1.5 times that of the unreinforced PAES foam to values of 1.5 GPa and 59 MPa, respectively. The CNF–PAES foam compared well with commercially available structural foams. The commercial structural foams that have high compressive properties have specific compressive moduli and strength values around 1.4 GPa and 70 MPa [1]. Shen et al. [14] observed an increase in the compressive properties, compared to the unreinforced polystyrene foam, when they foamed CNF reinforced polystyrene with CO_2 as the blowing agent. It was determined that during foaming, the CNFs aligned around the cell walls and helped to reinforce the walls during compression.

The specific compressive properties of the CNF–PAES foam were also affected by the foaming temperature. Similarly to the specific tensile modulus results, a higher release temperature, up to 220 °C, produced foam with greater specific compression modulus and strength than the lower release temperatures. As was argued for the tensile modulus, this increase was attributed to the greater cell wall thicknesses observed in the foam produced at 220 °C. However, at 227 °C the compressive properties were greatly decreased. The large reduction in the specific compressive properties is attributed to the inclusion of many macrocellular cells.

Table 1
Summary of the specific tensile, compressive, and impact properties for CNF–PAES foamed at varying release temperatures.

	Density (kg/m^3)	Specific tensile modulus (MPa)	Specific compressive modulus (MPa)	Specific compressive strength (MPa)	Specific impact strength (J/m)
Unfoamed CNF–PAES	1290	1105.7 ± 90.9	–	–	496.6 ± 66.4
CNF–PAES 165 °C	1087	622.0 ± 82.8	1222.9 ± 17.6	62.3 ± 3.7	137.8 ± 19.6
CNF–PAES 180 °C	730	600.6 ± 71.1	962.5 ± 95.1	43.1 ± 6.6	101.1 ± 36.6
CNF–PAES 200 °C	532	758.8 ± 92.6	1134.7 ± 188.3	58.7 ± 10.1	171.6 ± 50.0
CNF–PAES 220 °C	362	813.8 ± 98.1	1507.1 ± 188.0	58.7 ± 10.1	175.1 ± 50.9
CNF–PAES 227 °C	287	759.0 ± 171.9	948.2 ± 91.5	62.8 ± 5.2	188.2 ± 33.1
PAES 220 °C	245	936.1 ± 144.7	912.6 ± 60.2	38.8 ± 2.2	305.5 ± 55.6

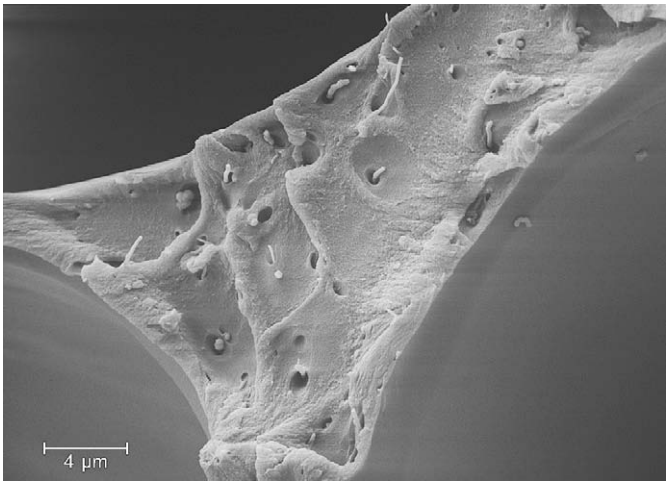

Fig. 8. SEM micrograph of CNF–PAES foamed with water and CO_2 at a release temperature of 220 °C. The presence of heterogeneous nucleation can be seen in the micrograph.

4. Conclusions

DMTA was demonstrated to be a more useful method than DSC to quantitatively determine the reduced T_g, due to plasticization, of the CNF–PAES saturated with water and CO_2. In the DMTA, two distinct T_gs were observed for the plasticized samples. The sharp peaks in the tan δ provided more quantitative results than in the DSC. The loss of the blowing agents yielded a large endothermic peak did the DSC thermograms, which overlapped with the reduced T_g, and hindered quantitatively determining the T_g.

The DMTA results were used to quantitatively determine the thermal transitions of the saturated polymer and yield a better understanding for choosing different foaming temperatures. The different foaming temperatures, corresponding to the thermal transitions observed in the DMTA, were chosen to control the cell morphology and foam density. Both the cell diameter and cell nucleation density were greatly affected by the temperature at which the pressure was released. As the temperature was increased, the cell size increased and the cell nucleation density decreased. The increase in the cell size was attributed to the longer cell growth times and cell coalescence. Cell coalescence accounts for the decrease in the cell nucleation density. The foam density

was also significantly affected by the temperature at which the pressure was released. At 165 °C, the foam density was the greatest because the cells did not have time to grow. At 227 °C, the cells had a longer time to grow and the foam density was reduced by 78%.

The addition of the CNFs where shown to greatly increase the compressive properties while slightly decreasing the impact strength of the foams. By adding in only 1% of the CNFs, both the specific compressive modulus and specific compressive strength were increased by over 1.5 times the modulus and strength of the unreinforced PAES foam. The specific compressive modulus and strength are greater than several commercial polymeric structural foams. However, the CNFs decreased the specific impact strength of the foams. By adding the CNFs to the PAES, the foam was much more rigid and less energy was absorbed by the sample bending during impact testing.

Acknowledgements

The authors would like to acknowledge the National Science Foundation IGERT (DMR-0114346) for partial funding. Parts of this work were carried out using instruments in the Nanoscale Characterization and Fabrication Laboratory, a Virginia Tech facility operated by the Institute for Critical Technology and Applied Science. The authors would also like to acknowledge the Wood Engineering Lab at Virginia Tech for use of the MTS compression testing machine and Christopher McGrady for his assistance with running the RMS-800.

References

[1] Marshall AC. Core composite and sandwich structures. In: Lee SM, editor. International encyclopedia of composites. VCH Publishers Inc.; 1990. p. 488–507.
[2] Altstädt V, Diedrichs F, Lenz T, Bardenhagen H, Jarnot D. Polym Polym Compos 1998;6(5):295–304.
[3] Martini-Vvedensky JE, Suh NP, Waldman FA. US patent 4,473,665; 1984.
[4] Collias DI, Baird DG. Polymer 1994;35(18):3978–83.
[5] Fu J, Naguib HE. J Cell Plast 2006;42:325–42.
[6] Manninen AR, Naguib HE, Nawaby AV, Liao X, Day M. Cell Polym 2005;24(2):49–70.
[7] Nam PH, Maiti P, Okamoto M, Kotaka T. Polym Eng Sci 2002;42(9):1907–18.
[8] Okamoto M, Nam PH, Maiti P, Kotaka T, Nakayama T, Takada M, et al. Nano Lett 2001;1(9):503–5.
[9] Lee YH, Wang KH, Park CB, Sain M. J Appl Polym Sci 2007;103:2129–34.
[10] Lee YH, Park CB, Wang KH. J Cell Plast 2005;41:486–502.
[11] Chang Y-W, Lee D, Bae S-Y. Polym Int 2006;55:184–9.
[12] Han X, Zeng C, Lee LJ, Koelling KW, Tomasko DL. Polym Eng Sci 2003;43(6):1261–75.
[13] Ray SS, Okamoto M. Prog Polym Sci 2003;28:1539–641.
[14] Shen J, Han X, Lee LJ. J Cell Plast 2006;42:105–26.
[15] Shen J, Zeng C, Lee LJ. Polym J 2005;46:5218–24.
[16] Sun H, Sur GS, Mark JE. Eur Polym J 2002;38:2373–81.
[17] Sun H, Mark JE. J Appl Polym Sci 2002;86:1692–701.
[18] VanHouten DJ, Baird DG. ANTEC 2008 – Proceedings of the 66th Annual Technical Conference & Exhibition. Milwaukee, WI: Society of Plastic Engineers, May 4–8, 2008. p. 1003–7.
[19] VanHouten DJ, Baird DG. Polym Eng Sci 2009;49(1):44–51.
[20] Kumar V, Weller JE. SPE ANTEC Tech Papers 1991;37:1401–5.
[21] Kumar V. Polym Eng Sci 1990;30(20):1323–9.
[22] Kumar V, Weller J. J Eng Ind 1994;116:413–20.
[23] Colton JS, Suh NP. Polym Eng Sci 1987;27(7):500–3.
[24] Fanegas N, Gomez MA, Jimenez I, Marco C, Garcia-Martinez JM, Ellis G. Polym Eng Sci 2008;48:80–7.